Fluorescent Indicators for Live-Cell and in Vitro Detection of Inorganic Cadmium Dynamics

Shulin Hu
South China University of Technology https://orcid.org/0000-0001-5042-3624
Jun Yang
South China University of Technology
Anqi Liao
South China University of Technology
Ying Lin
South China University of Technology
Shuli Liang (shuli@scut.edu.cn)
South China University of Technology https://orcid.org/0000-0002-9224-0049

Research Article

Keywords: inorganic cadmium, fluorescent indicator, live-cell, in vitro, dynamics, Escherichia coli, E. coli

Posted Date: December 6th, 2021

DOI: https://doi.org/10.21203/rs.3.rs-1103117/v1

Version of Record: A version of this preprint was published at Journal of Fluorescence on April 19th, 2022. See the published version at https://doi.org/10.1007/s10895-022-02919-0.

Abstract

Cadmium contamination is a severe threat to the environment and food safety. Thus, there is an urgent need to develop highly sensitive and selective cadmium detection tools. The engineered fluorescent indicator is a powerful tool for the rapid detection of inorganic cadmium in the environment. In this study, the development of yellow fluorescent indicators of cadmium chloride by inserting a fluorescent protein at different positions of the high cadmium-specific repressor and optimizing the flexible linker between the connection points is reported. These indicators provide a fast, sensitive, specific, high dynamic range, and real-time readout of cadmium ion dynamics in solution. Under optimal conditions, the fluorescent indicators N0C0/N1C1 showed a linear response to cadmium concentration within the range from 10/30 to 50/100 nM and with a detection limit of 10/33 nM. *Escherichia coli* cells containing the indicator were used to further study the response of cadmium ion concentration in living cells. *E. coli* N1C1 could respond to different concentrations of cadmium ions. This study provides a rapid and straightforward method for cadmium ion detection in vitro and the potential for biological imaging.

1 Introduction

Cadmium is a harmful heavy metal element. It is widely distributed in water, soil, and agricultural products, and spreads through the food chain to accumulate in the human body[1]. It causes great harm to the human body and has aroused widespread concern[2–4]. The intake of cadmium can adversely affect the kidneys, lungs, bone, and nervous system, with a biological half-life in the range of 17–30 years in the human body[5]. The long-term presence of cadmium causes renal dysfunction, calcium metabolism disorders, and an increased incidence of various diseases[6, 7]. For these reasons, it is vital to detect and quantify trace amounts of cadmium in environmental and food samples.

The traditional methods used to detect cadmium are mainly inductively coupled plasma mass spectrometry, atomic absorption spectroscopy and other techniques for sensitive detection[8]. However, these methods have disadvantages such as high cost, high technical difficulty, time-consuming sample pretreatment, inability to perform real-time detection, and the need for precision instruments[9–11].

A method based on the circularly permuted fluorescent protein (cpFP) gene-encoded fluorescent indicator can obtain a highly responsive sensor to make up for these shortcomings[12]. To obtain a sensor that is highly responsive to trace amounts of cadmium ions, the two ends of the cpFP, which is sensitive to small conformational changes and has a large fluorescence change range[13], are connected to the binding protein that can bind cadmium ions through a linker to obtain a new fluorescent protein so that the cadmium ions are bound to the binding protein and the conformation changes. The binding protein can easily drive the conformational change of the fluorescent protein, thus producing fluorescence changes[14, 15].

Therefore, the anti-cadmium operon CadR protein from *Pseudomonas putida* is a promising candidate for constructing a cadmium-specific sensor[16]. CadR is a homodimer composed of a DNA binding domain,

coiled coil domain, and a metal-binding domain (MBD). The unique triangular planar coordination formed by the three conserved cysteine residues of two monomers provides high selectivity and sensitivity to cadmium binding[16]. Under cadmium exposure, large conformational changes will occur in the MBD[17].

In the present study, we fused cpFP with the MBD of CadR to develop genetically encoded biosensors for inorganic cadmium. Then, we proved their excellent reversibility, high dynamic range, specificity for cadmium detection, and studied the response kinetics of cadmium in *E. coli*, which was helpful in determining the content of cadmium in vivo.

2 Materials And Methods

2.1 Materials and reagents

$CdCl_2$, $CoCl_2{\cdot}6H_2O$, $HgSO_4$, CuCl, and meso-2,3-Dimercaptosuccinic acid (DMSA) were all purchased from Macklin (Shanghai, China). KOD FX was purchased from Toyobo (Shanghai, China), and homologous recombinase was purchased from Clone Smarter (USA). T4 PNK ligase was purchased from Takara (Japan). In this study, other unspecified reagents were of analytical grade. CadR (NCBI: AF333961) was synthesized by GENEWIZ (Suzhou, China). pRSETB was from Invitrogen.

2.2 Construction of cadmium sensor

We ligated CadR[16] to pRSETB by homologous recombination, and then performed reverse PCR between the C112 to C119 amino acids of pRSETB-CadR (Table S1), and using the same method amplified cpYFP[18] with the homology arms at both ends of the insertion point of CadR the linkers SAG and GTG were added[19] (Table S2). Finally, the homologous recombinase was used for ligation for 15 mins at 50°C, and then transferred to *Escherichia coli* Top10 competent strain for amplification, and then extracted and sequenced. The plasmids identified by sequencing were introduced into *E. coli* BL21(DE3) competent cells, incubated overnight at 37°C, a single colony was picked to inoculate 100 ml of LB medium, and 0.1 mg/ml of ampicillin was added. Following culture for 8–12 hours at 37°C and 220 rpm to an OD_{600} of 0.4–0.6, 1 mM Isopropyl-beta-D-thiogalactopyranoside was added and incubated afor 20–24 hours t 18°C. The fermented strains were collected into HEPES buffer (100 mM HEPES, 100 mM NaCl) via ultrasonication, and the cell lysate supernatant was diluted with HEPES buffer, 0.5 μM, and 5 μM $CdCl_2$ were added, and the fluorescence intensity was immediately detected at $F_{485/528}$ and $F_{420/528}$.

To further optimize the cadmium sensor, we firstly knocked out the N-terminal methionine of cpYFP, and then used traditional truncation methods to shorten the amino acid linker between cpYFP and CadR to improve the response of $CadR_{16}$ (Table S3 and S4). First, we used reverse PCR to remove the amino acid linker at the N-terminus of cpYFP in $CadR_{16}$. The C-terminal linker was then reduced by the same method. In our nomenclature, N and C are the abbreviations for N-terminal and C-terminal, respectively. Therefore, N1C1 means that one amino acid at the N-terminal and C-terminal of the cpYFP linker have been removed

from $CadR_{16}$. All these truncated mutants were screened as described above. In addition, we changed the key cysteines C77, C112, and C119 of N0C0 to serine by site-directed mutagenesis (Table S5).

2.3 Protein expression and purification

We dissolved *E. coli* containing N0C0, N1C1, and C112S proteins in HEPES buffer and sonicated them on ice. These fusion proteins all had 6× His tags when they were constructed, and were purified by nickel-column affinity chromatography (Cytiva) on the AKTA pure system. The eluents were incubated with 10 mM EDTA at 4 ℃ to remove possible metal ions, such as nickel. Then, indicator proteins were concentrated using the Amicon Ultra centrifugal filter device (Millipore). A 5 ml desalting column (Cytiva) was then used to remove the imidazole and chelating agent contained in it, and was equilibrated with HEPES buffer (100 mM, 100 mM NaCl, pH 7.4) and then HEPES buffer (10 mM, 100 mM NaCl, pH 7.4). Protein concentrations were determined by the Bradford method using Coomassie Protein Assay Reagent with bovine serum albumin as the standard.

2.4 In vitro characteristics of the cadmium sensors

For spectrum measurement, the purified 0.2 μM N0C0 and N1C1 were added with or without 0.5/5 μM $CdCl_2$, and a microplate reader (TECAN infinite M200) was then used to measure the absorption spectrum at room temperature. The extinction coefficient was calculated with the Beer-Lambert equation according to the absorption spectrum. The fluorescence spectrum was detected with the emission wavelength fixed at 530 nm and the excitation wavelength at 400–550 nm; the excitation wavelength was fixed at 485 nm, the emission wavelength was 485–600 nm, and the scanning interval was 1 nm. To determine the quantum yield of purified N0C0 and N1C1, excitation was performed at the ultraviolet absorption peak, the emission spectrum was measured with a fluorescence spectrophotometer (Shimadzu RF-6000), and the integrated fluorescence value was calculated. EGFP (QY 0.60, pH 7.4)[20] was used as a control to calculate the quantum yield of N0C0. Similarly, the quantum yield of N1C1 was measured and calculated using the Brightness and Fluorescence Changes[21].

For all microplate experiments, the recombinant protein was diluted to a final concentration of 0.1–0.2 μM, and fluorescence was detected using the same settings as those for screening. In the Cd^{2+} titration experiment, 100 μL of different concentrations of Cd^{2+} and 100 μL of protein were mixed in a 96-well flat-bottomed plate, and the fluorescence change was immediately measured. All fluorescence intensities were normalized to a signal of 1 in the absence of cadmium at pH 7.4 and data were fitted to the Hill1 equation[22].

To determine the specificity of N0C0 and N1C1 against other ions, 100 μL of buffer containing different ionic components and 100 μL of purified protein were used for the reaction with or without 0.5/5 μM $CdCl_2$. The ion concentrations are listed below: 300 mM Na^+ or K^+, whereas other ions were 100 μM (Fe^{3+}, Mg^{2+}, Ca^{2+}, Ni^{2+}, Mn^{2+}, Fe^{2+}, Li^+, Cs^+, Ba^{2+}, Co^{2+}) or 0.5 μM (Ag^+, Zn^{2+}, Cu^{2+}, Pb^{2+}, Hg^+, Cu^+). To determine the sensitivity of N0C0 and N1C1 to temperature, a 25–40°C temperature program in a microplate reader was performed and the fluorescence change was detected every 20 seconds. To determine the

dependence of N0C0 and N1C1 on the pH value, HEPES buffer with a pH value ranging from 6.8 to 8.4 was prepared at 0.2 pH unit intervals.

At the same time, in order to study the in vitro response kinetics of N0C0 and N1C1, 0.5/5 μM Cd^{2+} and 2 mM DMSA were sequentially added, and the fluorescence changes were monitored every 20 seconds.

2.5 Measuring inorganic cadmium in *E. coli*

E. coli cells after fermentation were washed and dissolved in HEPES buffer, the bacterial solution was diluted to an OD_{600} of 1, the microplate reader was set to 37°C and incubated for 5 min, and 0.5/5 μM Cd^{2+} and 2 mM DMSA were sequentially added. The fluorescence changes were detected every 60 seconds.

2.6 Data analysis

Unless otherwise specified in this study, data processing was normalized, and the ratio of excitation at 485 nm, excitation at 420 nm, and emission at 528 nm ($R_{485/420}$) are presented. The data are presented as a representative example of a single experiment repeated three or more times. The data obtained are expressed as mean ± SD or mean ± SEM.

3 Results And Discussion

3.1 Synthesis of cpFP-based cadmium sensor

To obtain a cadmium ion sensor, we firstly amplified CadR onto the vector pRSETB and then inserted cpYFP between the key residues Cys112 and Cys119 of the MBD domain of the CadR protein with two flexible linkers, SAG and GTG, by homologous recombination; thus, 28 chimeras were produced (Fig. 1a).

After fermenting and expressing each chimera, the chimera ($CadR_{16}$) with cpYFP inserted between the Ala114 and Ala117 of the MBD showed an approximately 200% increase in the ratio of fluorescence when excited at 485 nm and 420 nm when 5 μM Cd^{2+} was added (Fig. 1b). Compared with the other 27 chimeras, $CadR_{16}$ had a higher response level to Cd^{2+}, so we used $CadR_{16}$ as our subsequent optimization model.

Therefore, to further expand the dynamic range of the detection of cadmium ions, we deleted the starting amino acid methionine of cpYFP, and based on this, reduced the number of amino acids in the linker, and constructed a total of 16 truncation variants (Fig. 1c). We used the same method and found that N0C0/N1C1 in the presence of 0.5 μM/5 μM Cd^{2+}, when excited at 485 nm and 420 nm, showed an approximately 230% increase and 167% decrease in fluorescence, respectively (Fig. 1d). After the three key cysteine residues (C77/C112/C119) were mutated to serine, no obvious fluorescence changes were observed for the non-functional control, under cadmium exposure (Fig. 1d). These results indicated that the response of N0C0 and N1C1 to cadmium ions was caused by the binding of cadmium to cysteine in

the MBD domain of the CadR protein. These data indicated that N0C0 and N1C1 are sensors with high response and high sensitivity to cadmium ions, and they are promising tools for in vitro detection.

3.2 In vitro characterization of the cadmium sensor based on cpFP

We characterized the spectral and biochemical properties of the purified N0C0 and N1C1 in a cadmium and cadmium-free environment. N0C0 and N1C1 had excitation peaks near 500 nm and emission peaks near 515 nm in the fluorescence spectrum, and absorption peaks near 410 nm and 500 nm in the ultraviolet spectrum, respectively (Fig. 2, Table 1). In addition, we measured the extinction coefficient and quantum yield of N0C0 and N1C1, the quantum yield of N0C0 and N1C1 was about 3.3% and 30% of EGFP when excited at 410 nm and 500 nm. The molecular brightness change in N0C0 and N1C1, defined as the ratio of the brightness change with or without Cd^{2+}, increased 229% and decreased 151%, respectively (Table 1). Protein titration experiments showed that by fitting the Hill1 equation, the apparent Cd^{2+} dissociation constants (K_d) of N0C0 and N1C1 were 0.12 μM and 0.10 μM, respectively (Fig. 3a-b, Table 1). We performed a linear fit to the titration experiment. N0C0 and N1C1 had a linear range from 0.01 μM to 0.05 μM and from 0.03 μM to 0.1 μM, and the limit of detection (LOD) was 10 nM and 33 nM, respectively. The low detection limit was due to the ability of CadR protein to bind cadmium ions and the ability of the fluorescent protein to make changes in autofluorescence to weak conformational changes, demonstrating that the indicator can measure low concentrations of cadmium ions.

Table 1
Properties of cadmium sensors

Sensor	$CdCl_2$ (μM)	λ_{abs}	ε	λ_{em}	QY	Brightness	Change	K_d (μM)	LOD (nM)
N0C0	-	410	18.8	511	0.0197	0.37	2.29	0.12	10
		499	10.6	517	0.1613	1.71			
	+	410	16.7	512	0.0219	0.37			
		499	20.2	516	0.1939	3.92			
N1C1	-	412	18.7	511	0.0182	0.34	0.66	0.10	33
		497	13.5	517	0.1519	2.05			
	+	412	28.4	513	0.0173	0.49			
		497	12	517	0.1622	1.95			

Note Photophysical properties of N0C0/N1C1 with or without cadmium were measured at room temperature. Extinction coefficients (ε, $mM^{-1} \cdot cm^{-1}$) were calculated from absorbance (abs) spectra. QYs of N0C0 and N1C1 were measured against EGFP at pH 7.4 (QY 0.6). Brightness is defined as the product of extinction coefficient and quantum yield. Experimental data were fitted to Hill1 equation.

The ion specificity experiments conducted showed that N0C0 and N1C1 have similar properties for the specificity of metal ions. Among them, Ni^{2+}, Ag^{+}, Cu^{2+}, $Cu^{+,}$ and Co^{2+} all had an inhibitory effect on the properties of the protein, and there was a competitive relationship between Zn^{2+} and Cd^{2+} (Fig. 3c–d). These sensors did not respond to different concentrations of hydrogen peroxide (Fig. 3e).

In addition, N0C0 and N1C1 could detect Cd^{2+} at different temperatures (25–40 ℃), which showed that they had temperature adaptability (Fig. 4a-b). Similar to other cpFP fluorescent probes[14, 18], the fluorescence of N0C0 and N1C1 was affected by pH. With an increase in pH, the fluorescence level of F_{485} increased continuously (Fig. 4c–d).

Kinetic studies showed that the addition of Cd^{2+} to N0C0 resulted in an immediate reaction and reached a maximum within 200 seconds (Fig. 5a), while N1C1 reached a maximum immediately (Fig. 5b). When DMSA was added, it responded immediately and returned to the normal level (Fig. 5a–b), which showed its reversibility in real-time detection.

3.3 Sensitivity of the cadmium sensor to cadmium in *E. coli*

We studied the cadmium sensing properties of N0C0 and N1C1 expressed in the cytoplasm of *E. coli*. Similarly, we carried out titration experiments with *E. coli* containing N0C0 and N1C1 and added 0.5/5 μM Cd^{2+} to *E. coli*, and then exposed the bacterial cells to 2 mM DMSA. The N0C0 *E. coli* cells did not respond to cadmium ions in both the titration and kinetic experiments (Fig. 5c and e). The N1C1 *E. coli* cells showed similar responsiveness to different cadmium ion concentrations in the titration experiment as the purified protein (Fig. 5d). The N1C1 *E. coli* cells supplemented with Cd^{2+} produced changes in fluorescent signals. N1C1 continued to combine with Cd^{2+} until DMSA was added to combine with Cd^{2+}, thereby releasing part of the sensor (Fig. 5f). Compared with the titration solution, the different responses of N0C0 and N1C1 to Cd^{2+} may be attributed to the limited entry rate of cadmium through thick cell walls and plasma membranes, as well as the influence of *E. coli* cadmium resistance and adsorption capacity to cadmium ions[23].

4 Conclusion

In summary, we engineered genetically encoded yellow fluorescent indicators based on the gene encoding of *P. putida* CadR by constantly changing the insertion point strategies and optimization methods of deleting amino acid linkers. A total of 28 chimeras and 16 deletions were constructed. Their properties as purified proteins were characterized to measure the changes in inorganic cadmium in vitro.

N0C0/N1C1 showed marked sensitivity and specificity to cadmium ions and can quantify cadmium ions in real-time. N0C0 reached the maximum fluorescence change of 200% under the reaction of 0.5 μM cadmium ion concentration in 2 minutes, and N1C1 reached the maximum fluorescence change of 167% immediately under the reaction of 5 μM cadmium ion concentration. Compared with the FRET model Met-cad 1.57 cadmium ion sensor, N0C0 and N1C1 have a larger dynamic range[24]. The sensor showed wide

linearity in the concentration range of 0.01–0.05 μM, and the LOD of N0C0 and N1C1 was 10 nM and 33 nM, respectively. Compared with other types of developed sensors, including electrochemistry, Schiff base and otherwise (Table 2). The LOD of N0C0/N1C1 showed better or equivalent detection sensitivity. Moreover, the preparation of the fluorescent indicator was simple, the detection was convenient, and the detection speed was fast.

Table 2

Comparison of detection performances among different assays for Cd^{2+} detection

Name	Linear range (nM)	LOD (nM)	Detection method	Ref.
N0C0	10-50	10	Fluorescence	This study
N1C1	30-100	33	Fluorescence	This study
p2T7RNAPmut-68	-	10	WCBs	[25]
phosphorescence sensor	0.44-44.5	0.36	phosphorescence	[26]
DMBA	-	102	Schiff	[27]
GCDSA	-	0.15	DNA probes	[28]
probe 1	-	114	Schiff	[29]
MIL-101(Cr)	0.9-27	0.5	electrochemical	[30]
nanoparticles-modified chemical sensor	2.7-222	0.5	electrochemical	[31]
paper sensor	-	44	immunochromatographic	[32]
L-cysteine functionalized gold–silver nanoparticles	400-38600	44	colorimetric	[33]
CdS QDs	62.5-1250	10	Fluorescence	[34]

The developed cadmium sensors can easily be used for the quantitative measurement of Cd^{2+} in solution, because the purified Cd^{2+} sensor protein is added to the solution containing Cd^{2+}, and its fluorescence change can be easily detected with a microplate reader.

N0C0 and N1C1 have the potential to be used in the real-time, quantitative measurement of single cells and subcellular trends. The detection of Cd^{2+} content in living organisms is very useful for research on the toxicity of cadmium in living cells or in vivo. Moreover, CadR is a class of proteins belonging to the MerR family. This indicator can provide a theoretical basis for the detection of metal ions in other MerR families, including Zn^{2+}, Cu^{2+}, Pb^{2+}.

Declarations

Acknowledgements

The authors are grateful for the following support: We thank Dr.Yuzheng Zhao, East China University of Science and Technology, for providing the cpYFP plasmid.

Funding：This work was supported by Guangdong Key Area Research and Development Program (Grant No. 2019B020210003) and the National Key Research and Development Program (2018YFA0901700).

Competing Interests：The authors have no relevant financial or non-financial interests to disclose.

Authors' Contributions：Shulin Hu conducted the experiment and drafted the manuscript, Jun Yang analyzed the results, Anqi Liao experiment assisted. All authors read and approved the final manuscript.

Data Availability: All data generated or analyzed during this study are included in this published article and its supplementary information

Ethics Approval : Not applicable.

Consent to Participate : Not applicable.

Consent to Publication : Not applicable.

Conflicts of interest/Competing Interests : the authors declare no conflicts of interest or competing interests.

References

1. Williams C, D. David (1973) The effect of superphosphate on the cadmium content of soils and plants. Soil Research 11(1):43–56. https://doi.org/10.1071/SR9730043
2. Zou J, Zhang Y, Li X, Ma X, Liu J, Peng X, Sun Z (2021) Sexual differences in root growth and antioxidant characteristics in Salix viminalis exposed to cadmium stress. Int J Phytoremediation. https://doi.org/10.1080/15226514.2021.1904825
3. Zha YQ, Zhang KK, Pan F, Liu X, Han SM, Guan P (2021) Cloning of PCS gene (TpPCS1) from Tagetes patula L. and expression analysis under cadmium stress. Plant Biol 23(3):508–516. https://doi.org/10.1111/plb.13207
4. Hou Q, Ma A, Wang T, Lin J, Wang H, Du B, Zhuang X, Zhuang G (2015) Detection of bioavailable cadmium, lead, and arsenic in polluted soil by tailored multiple Escherichia coli whole-cell sensor set. Anal Bioanal Chem 407(22):6865–6871. https://doi.org/10.1007/s00216-015-8830-z
5. Fatima G, Raza AM, Hadi N, Nigam N, Mahdi AA (2019) Cadmium in Human Diseases: It's More than Just a Mere Metal. Indian J Clin Biochem 34(4):371–378. https://doi.org/10.1007/s12291-019-00839-8

6. Waisberg M, Joseph P, Hale B, Beyersmann D (2003) Molecular and cellular mechanisms of cadmium carcinogenesis. Toxicology 192(2–3):95–117. https://doi.org/10.1016/s0300-483x(03)00305-6
7. Wang JH, Liu YM, Chao JB, Wang H, Wang Y, Shuang SM (2020) A simple but efficient fluorescent sensor for ratiometric sensing of Cd2+ and bio-imaging studies. Sensor Actuator B-Chem 303:127216. https://doi.org/10.1016/j.snb.2019.127216
8. Maghsoudi AS, Hassani S, Mirnia K, Abdollahi M (2021) Recent Advances in Nanotechnology-Based Biosensors Development for Detection of Arsenic, Lead, Mercury, and Cadmium. Int J Nanomed 16:803–832. https://doi.org/10.2147/ijn.S294417
9. Cui L, Wu J, Ju H (2015) Electrochemical sensing of heavy metal ions with inorganic, organic and bio-materials. Biosensors and Bioelectronics 63:276–286. https://doi.org/10.1016/j.bios.2014.07.052
10. Kim HJ, Lim JW, Jeong H, Lee SJ, Lee DW, Kim T, Lee SJ (2016) Development of a highly specific and sensitive cadmium and lead microbial biosensor using synthetic CadC-T7 genetic circuitry. Biosens Bioelectron 79:701–708. https://doi.org/10.1016/j.bios.2015.12.101
11. Li L, Liang J, Hong W, Zhao Y, Sun S, Yang X, Xu A, Hang H, Wu L, Chen S (2015) Evolved Bacterial Biosensor for Arsenite Detection in Environmental Water. Environ Sci Technol 49(10):6149–6155. https://doi.org/10.1021/acs.est.5b00832
12. Helassa N, Zhang X-h, Conte I, Scaringi J, Esposito E, Bradley J, Carter T, Ogden D, Morad M, Toeroek K (2015) Fast-Response Calmodulin-Based Fluorescent Indicators Reveal Rapid Intracellular Calcium Dynamics. Sci Rep 5. https://doi.org/10.1038/srep15978
13. Liu WF, Deng MY, Yang CM, Liu F, Guan XM, Du YC, Wang L, Chu J (2020) Genetically encoded single circularly permuted fluorescent protein-based intensity indicators. J Phys-D-Appl Phys 53(11):22. https://doi.org/10.1088/1361-6463/ab5dd8
14. Tao R, Shi M, Zou Y, Cheng D, Wang Q, Liu R, Wang A, Zhu J, Deng L, Hu H, Chen X, Du J, Zhu W, Zhao Y, Yang Y (2018) Multicoloured fluorescent indicators for live-cell and in vivo imaging of inorganic mercury dynamics. Free Radical Biol Med 121:26–37. https://doi.org/10.1016/j.freeradbiomed.2018.04.562
15. Zhao Y, Hu Q, Cheng F, Su N, Wang A, Zou Y, Hu H, Chen X, Zhou HM, Huang X, Yang K, Zhu Q, Wang X, Yi J, Zhu L, Qian X, Chen L, Tang Y, Loscalzo J, Yang Y (2015) SoNar, a Highly Responsive NAD+/NADH Sensor, Allows High-Throughput Metabolic Screening of Anti-tumor Agents. Cell Metab 21(5):777–789. https://doi.org/10.1016/j.cmet.2015.04.009
16. Lee SW, Glickmann E, Cooksey DA (2001) Chromosomal locus for cadmium resistance in Pseudomonas putida consisting of a cadmium-transporting ATPase and a MerR family response regulator. Appl Environ Microbiol 67(4):1437–1444. https://doi.org/10.1128/AEM.67.4.1437-1444.2001
17. Liu X, Hu Q, Yang J, Huang S, Wei T, Chen W, He Y, Wang D, Liu Z, Wang K, Gan J, Chen H (2019) Selective cadmium regulation mediated by a cooperative binding mechanism in CadR. Proc. Natl.

Acad. Sci. U. S. A. 116(41) 20398-20403. https://doi.org/10.1073/pnas.1908610116

18. Zhao Y, Jin J, Hu Q, Zhou HM, Yi J, Yu Z, Xu L, Wang X, Yang Y, Loscalzo J (2011) Genetically encoded fluorescent sensors for intracellular NADH detection. Cell Metab 14(4):555–566. https://doi.org/10.1016/j.cmet.2011.09.004
19. Belousov VV, Fradkov AF, Lukyanov KA, Staroverov DB, Shakhbazov KS, Terskikh AV, Lukyanov S (2006) Genetically encoded fluorescent indicator for intracellular hydrogen peroxide. Nat Methods 3(4):281–286. https://doi.org/10.1038/nmeth866
20. Patterson GH, Knobel SM, Sharif WD, Kain SR, Piston DW (1997) Use of the green fluorescent protein and its mutants in quantitative fluorescence microscopy. Biophys J 73(5):2782–2790. https://doi.org/10.1016/s0006-3495(97)78307-3
21. Subach OM, Barykina NV, Chefanova ES, Vlaskina AV, Sotskov VP, Ivashkina OI, Anokhin KV, Subach FV (2021) FRCaMP, a Red Fluorescent Genetically Encoded Calcium Indicator Based on Calmodulin from Schizosaccharomyces Pombe Fungus. Int J Mol Sci 22(1). https://doi.org/10.3390/ijms22010111
22. Barykina NV, Subach OM, Piatkevich KD, Jung EE, Malyshev AY, Smirnov IV, Bogorodskiy AO, Borshchevskiy VI, Varizhuk AM, Pozmogova GE, Boyden ES, Anokhin KV, Enikolopov GN, Subach FV (2017) Green fluorescent genetically encoded calcium indicator based on calmodulin/M13-peptide from fungi. PLoS ONE 12(8). https://doi.org/10.1371/journal.pone.0183757
23. Qin W, Liu X, Yu X, Chu X, Tian J, Wu N (2017) Identification of cadmium resistance and adsorption gene from Escherichia coli BL21 (DE3). RSC Adv 7(81):51460–51465. https://doi.org/10.1039/c7ra10656d
24. Chiu TY, Chen PH, Chang CL, Yang DM (2013) Live-cell dynamic sensing of Cd(2+) with a FRET-based indicator. PLoS ONE 8(6):e65853. https://doi.org/10.1371/journal.pone.0065853
25. Jia X, Liu T, Ma Y, Wu K (2021) Construction of cadmium whole-cell biosensors and circuit amplification. Appl Microbiol Biotechnol. https://doi.org/10.1007/s00253-021-11403-x
26. Lai B, Wang R, Yu X, Wang H, Wang Z, Tan M (2020) A Highly Sensitive "on-off" Time-Resolved Phosphorescence Sensor Based on Aptamer Functionalized Magnetite Nanoparticles for Cadmium Detection in Food Samples. Foods 9(12). https://doi.org/10.3390/foods9121758
27. Aydin Z, Keles M (2020) Colorimetric cadmium ion detection in aqueous solutions by newly synthesized Schiff bases. Turk J Chem 44(3):791–804. https://doi.org/10.3906/kim-1912-36
28. Zuou B, Chen Y-T, Yang X-Y, Wang Y-S, Hu X-J, Suo Q-L (2019) An Ultrasensitive Colorimetric Strategy for Detection of Cadmium Based on the Peroxidase-like Activity of G-Quadruplex-Cd(II) Specific Aptamer. Anal Sci 35(3):277–282. https://doi.org/10.2116/analsci.18P248
29. Zehra S, Khan RA, Alsalme A, Tabassum S (2019) Coumarin Derived "Turn on" Fluorescent Sensor for Selective Detection of Cadmium (II) Ion: Spectroscopic Studies and Validation of Sensing Mechanism by DFT Calculations. J Fluoresc 29(4):1029–1037. https://doi.org/10.1007/s10895-019-02416-x

30. Shi E, Yu G, Lin H, Liang C, Zhang T, Zhang F, Qu F (2019) The incorporation of bismuth(III) into metal-organic frameworks for electrochemical detection of trace cadmium(II) and lead(II). Microchim Acta 186(7). https://doi.org/10.1007/s00604-019-3522-6
31. Wang N, Kanhere E, Miao J, Triantafyllou MS (2018) Nanoparticles-Modified Chemical Sensor Fabricated on a Flexible Polymer Substrate for Cadmium(II) Detection. Polymers 10(7) https://doi.org/10.3390/polym10070694
32. Song S, Zou S, Zhu J, Liu L, Kuang H (2018) Immunochromatographic paper sensor for ultrasensitive colorimetric detection of cadmium. Food Agric Immunol 29(1):3–13. https://doi.org/10.1080/09540105.2017.1354358
33. Du J, Hu X, Zhang G, Wu X, Gong D (2018) Colorimetric detection of cadmium in water using L-cysteine Functionalized gold-silver nanoparticles. Anal Lett 51(18):2906–2919. https://doi.org/10.1080/00032719.2018.1455103
34. Tang X, Wang J, Zhao K, Xue H, Ta C (2016) A Simple and Rapid Label-free Fluorimetric "Turn Off-on" Sensor for Cadmium Detection Using Glutathione-capped CdS Quantum Dots. Chem Res Chin Univ 32(4):570–575. https://doi.org/10.1007/s40242-016-5448-4

Figures

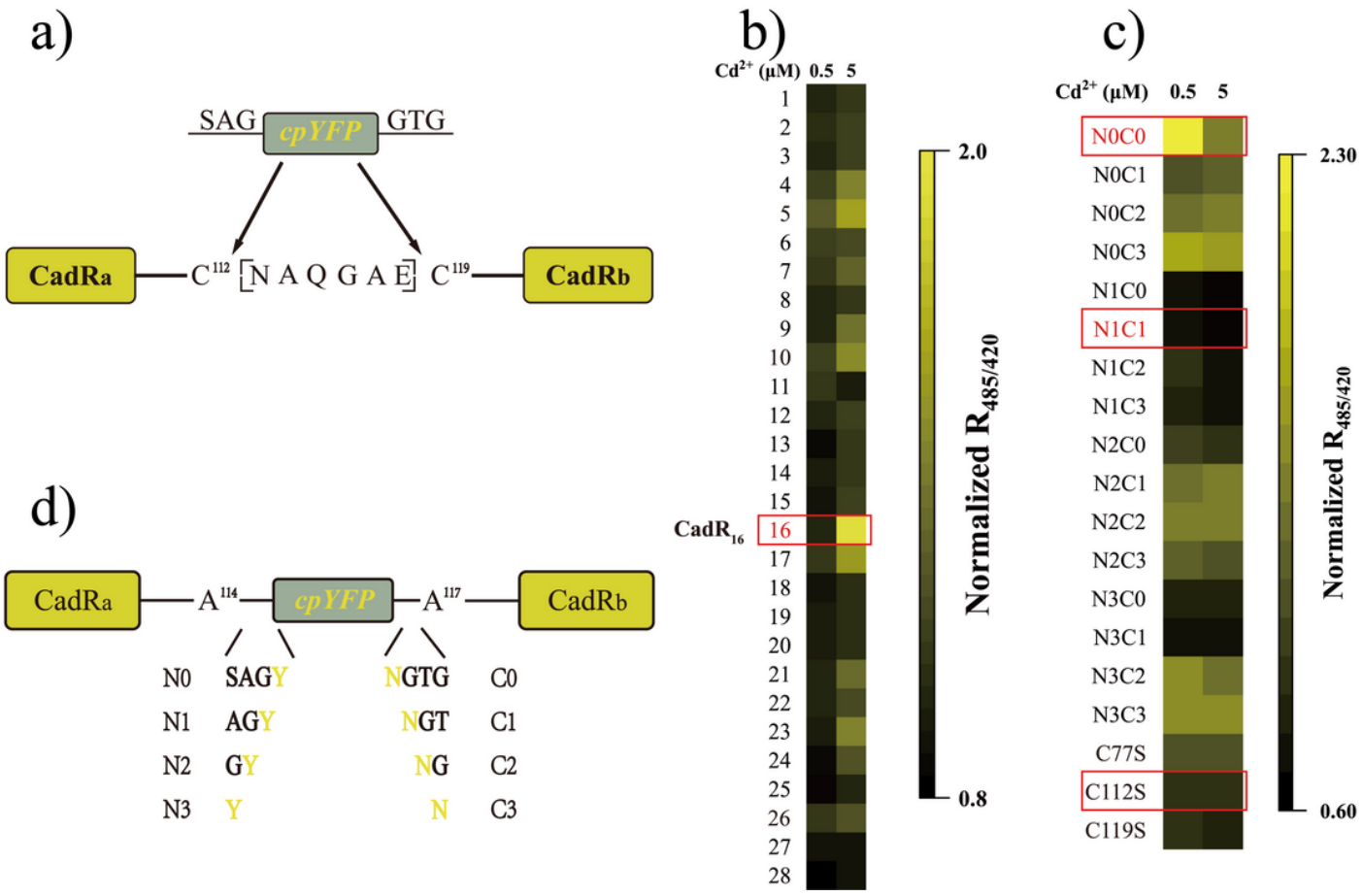

Figure 1

Generation of a cadmium sensor based on the cpFP type. (a) The construction model of the cadmium sensor of the chimera. (b) Fluorescence response of the constructed cadmium sensor chimera under 0.5 μM and 5 μM CdCl2. (c) The construction model of the cadmium sensor with the cut-off sub. (d) Fluorescence response of the constructed cadmium sensor cut-off at 0.5 μM and 5 μM CdCl2

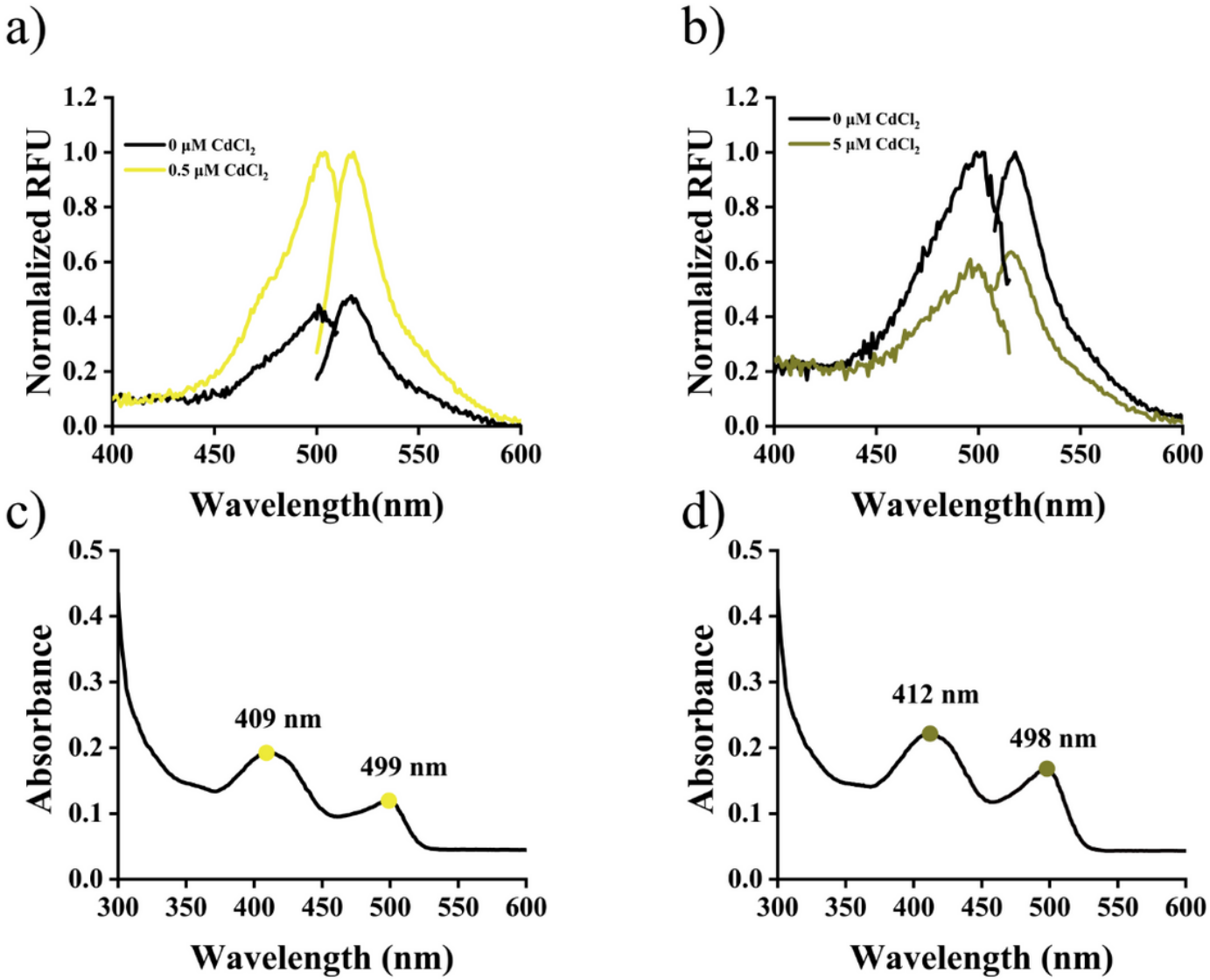

Figure 2

The optical properties of the cadmium sensor in vitro. (a and b) Fluorescence spectra of purified N0C0 (a) and N1C1 (b). The fluorescence spectrum intensity of purified and desalted N0C0 and N1C1 were measured under blank conditions and after the addition of 0 μM and 0.5 μM CdCl2. The fixed wavelength of excitation was 485 nm, and the fixed wavelength of emission was 550/530 nm, and the scanning interval was 1 nm. The fluorescence maximum value was used for normalization. (c and d) UV spectra of purified N0C0 (c) and N1C1 (d). The purified N0C0 and N1C1 were scanned for UV spectra at 300–600 nm. The scanning interval was 1 nm

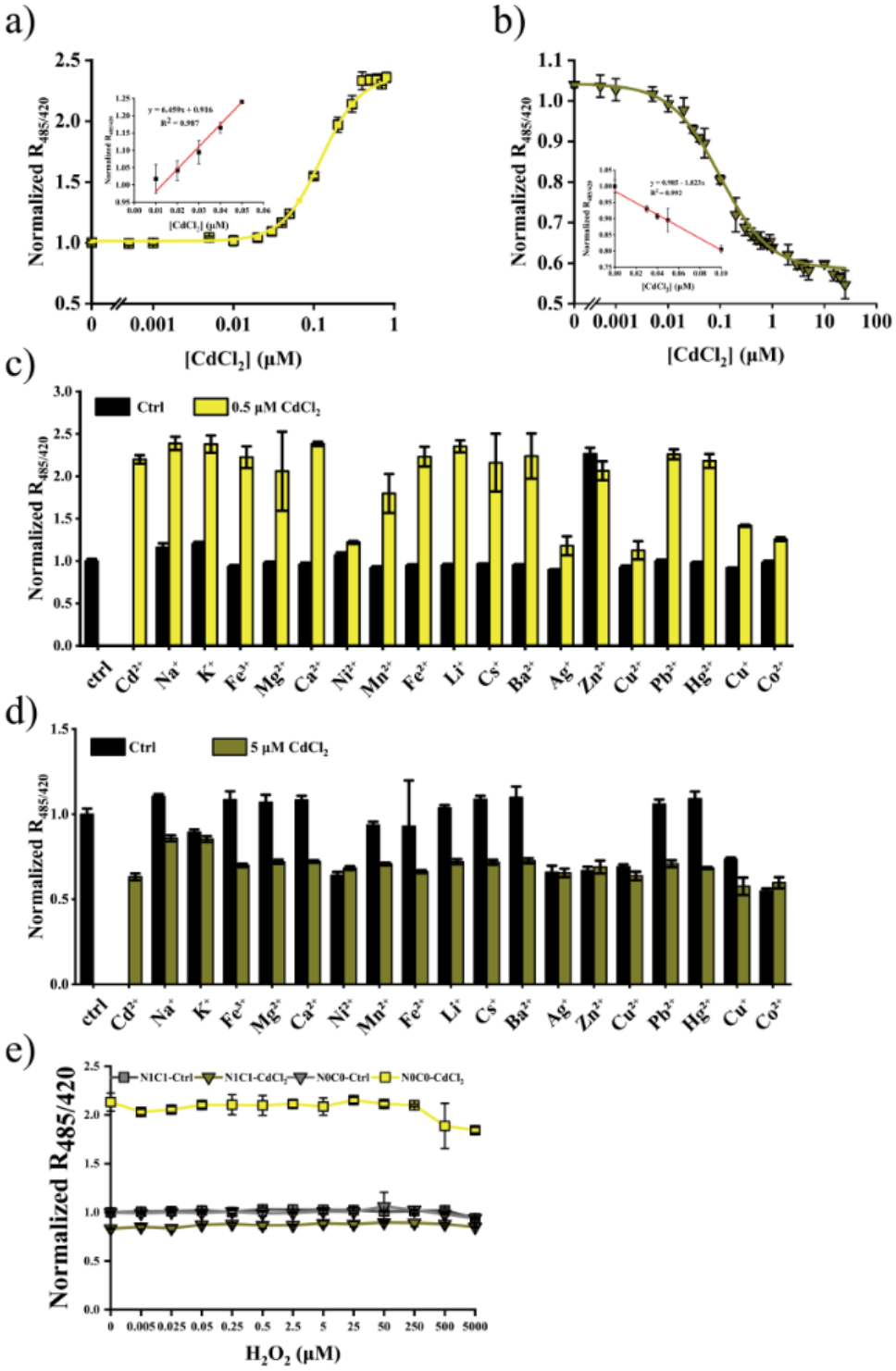

Figure 3

In vitro characterization of cadmium sensors. (a and b) Fluorescence titration curves of N0C0 (a) and N1C1 (b). The excitation ratios (R485/420) of N0C0/N1C1 were normalized to control conditions in the absence of cadmium. (c and d) Metal specificity of N0C0 (c) and N1C1 (d). Fluorescence changes toward or in the presence of other metal ions. (e) Hydrogen peroxide (H2O2) specificity of N0C0 and N1C1. Fluorescence changes toward or in the presence of H2O2

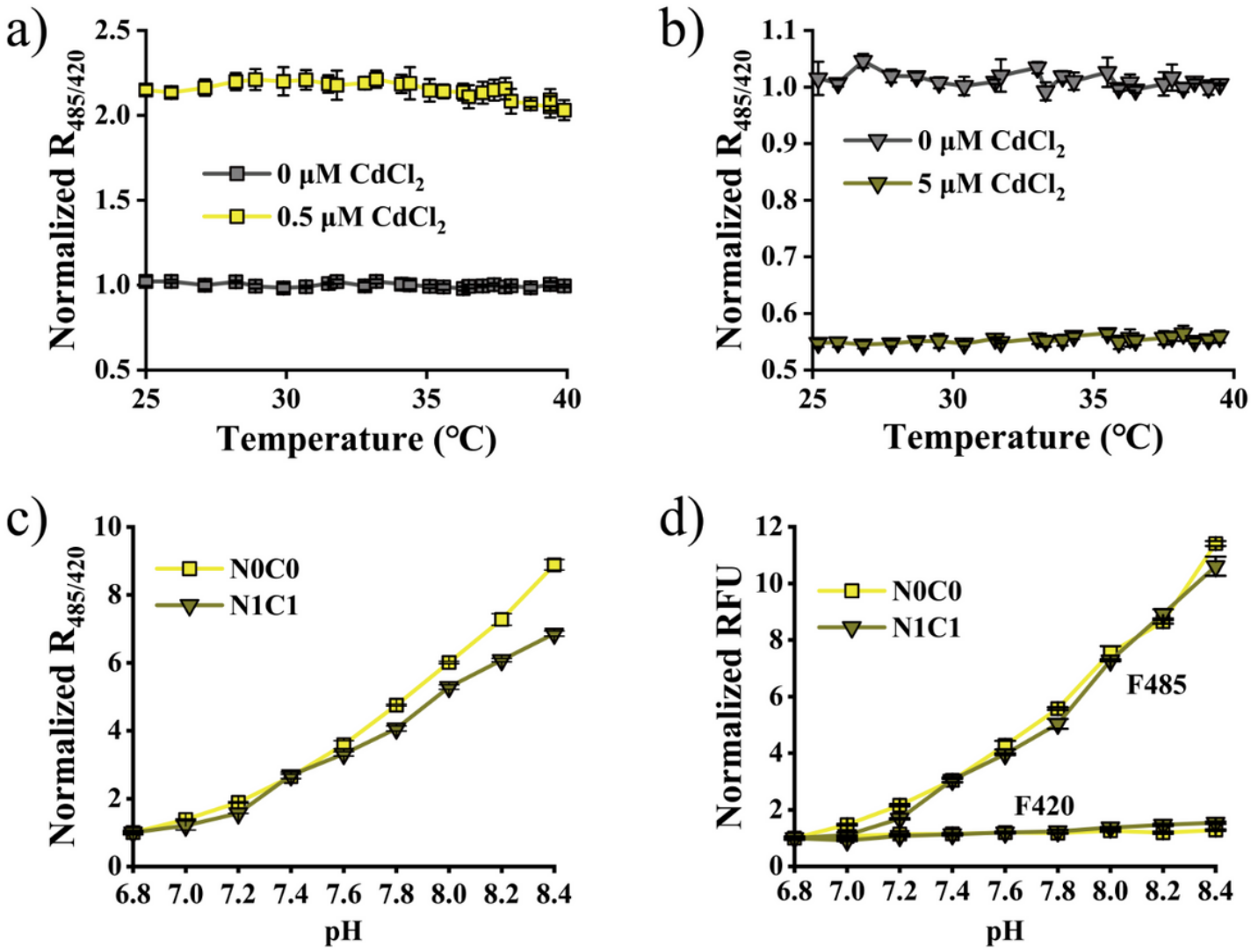

Figure 4

The temperature and pH sensitivity of cadmium sensors. (a and b) Temperature sensitivity of N0C0 (a) and N1C1 (b). The fluorescence changes of N0C0 and N1C1 at 25–40 °C in the presence/absence of cadmium ions. (c) pH dependency of N0C0 and N1C1 was similar. (d) Fluorescence of N0C0 and N1C1 with excitation at 420 nm or 485 nm at the indicated pH

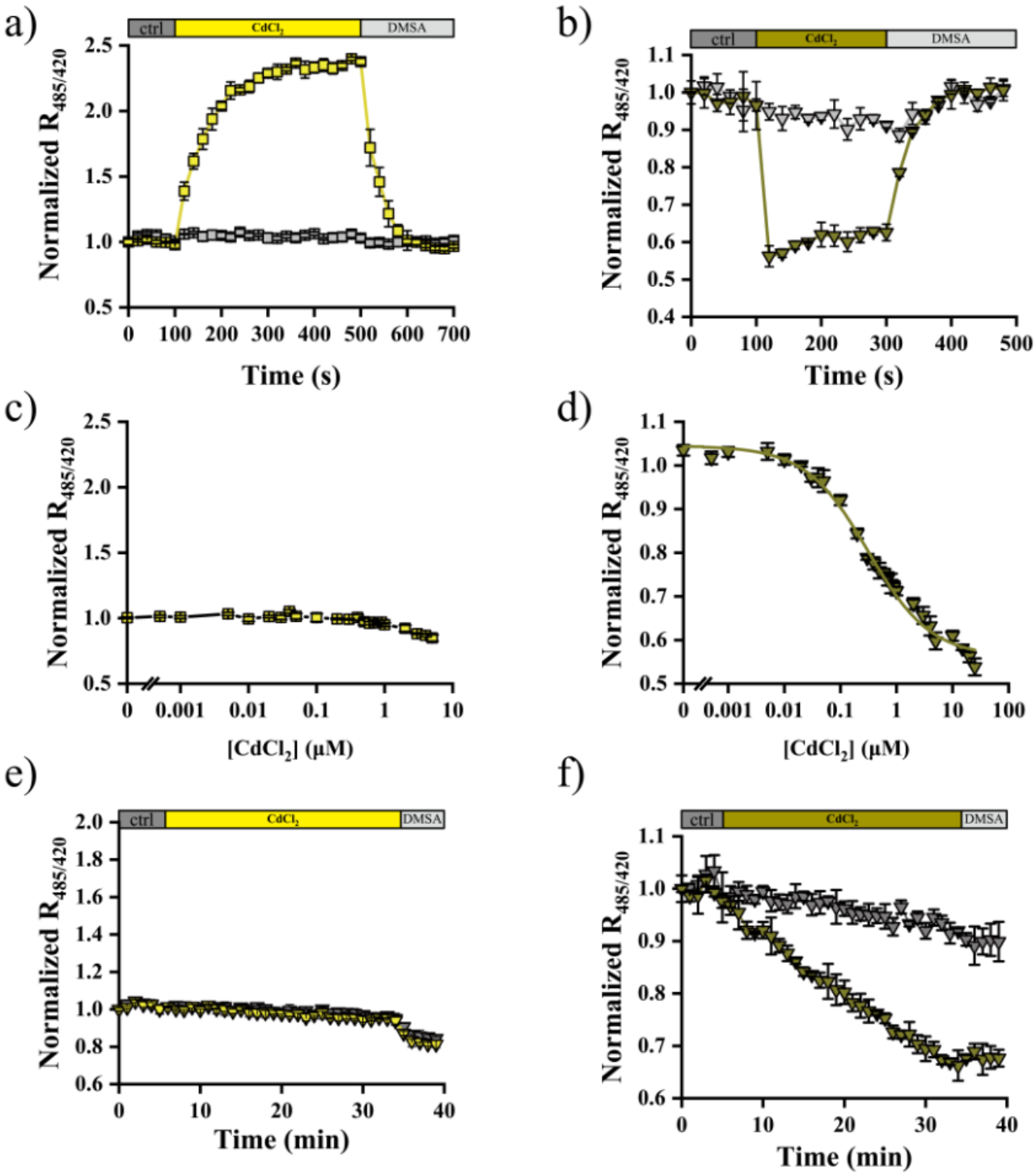

Figure 5

Monitoring Cd2+ dynamics in vitro and in living bacteria. (a and b Kinetics of fluorescence response of purified N0C0 (a) and N1C1 (b) to the sequential addition of CdCl2 and DMSA. (c and d) Fluorescence response of N0C0 (c) and N1C1 (d) in E. coli BL21(DE3) treated with exogenous CdCl2. Cells were treated with different concentrations of CdCl2 for 30 minutes at 37 °C. (e and f) Fluorescence change of N0C0 (e) and N1C1 (f) in response to 0.5/5 μM CdCl2 and its chelator DMSA (2 mM) in E. coli BL21(DE3)

Supplementary Files

This is a list of supplementary files associated with this preprint. Click to download.

- Supplementarymaterials.pdf